In vivo evaluation of the antiviral effect of ClO_2 in chicken embryos inoculated with avian infectious bronchitis coronavirus

Zambrano-Estrada, Xóchitl[a], Domínguez-Sánchez, Carlos[b], Banuet-Martínez, Marina[b], Guerrero de la Rosa, Fabiola[b], García-Gasca, Teresa[c], Acevedo-Whitehouse, Karina[b]

[a] Laboratory of Veterinary Diagnostic Pathology. School of Natural Sciences. Autonomous University of Queretaro. Av. De las Ciencias S/N. Juriquilla, Queretaro. Qro. C.P.76230. Mexico,

[b] Unit for Basic and Applied Microbiology. School of Natural Sciences. Autonomous University of Queretaro. Anillo Vial Fray Junípero Serra, Querétaro, Qro. C.P. 76140

[c] Laboratory of Cellular Biology. School of Natural Sciences. Autonomous University of Queretaro. Av. De las Ciencias S/N. Juriquilla, Queretaro. Qro. C.P. 76230. Mexico

Corresponding author: Karina Acevedo-Whitehouse (karina.acevedo.whitehouse@uaq.mx)

Abstract

The need for safe and effective antiviral treatments is pressing, particularly given the number of viral infections that are prevalent in animal and human populations, often causing devastating economic losses and mortality. In the context of the current coronavirus pandemic, which has highlighted how devastating the effects of a virus can be on a naïve population, it is imperative to have rigorous and unbiased data on the efficacy and safety of potential antiviral treatments, particularly those that have demonstrated virucidal effects as a disinfectant, are being considered for use despite warnings on their potential toxicity, but no not have empirical evidence of their antiviral effect *in vivo*. Here, we tested the effect of chlorine dioxide (ClO_2) on chick embryos infected with avian infectious bronchitis coronavirus (IBV). We determined virus-induced mortality on 10-day old embryos inoculated with 10^4 mean EID_{50}/mL of attenuated Massachusetts and Connecticut IBV strains. We determined viral titres using RT-qPCR and conducted histopathological examination of various tissues and organs. Viral titres were 2.4-fold lower and mortality was reduced by half in infected embryos that were treated with ClO_2. Infection led to developmental abnormalities regardless of treatment. Lesions typical of IBV infections were observed in all inoculated embryos, but severity tended to be lower in ClO_2-treated embryos. We found no gross or microscopic evidence of toxicity caused by ClO_2 at the doses used herein. Our study shows that ClO_2 could be a safe and viable option for controlling avian coronavirus, and raises the possibility that similar effects could be observed in other organisms.

Keywords

Chlorine dioxide, ClO_2, coronavirus, IBV, antiviral, chick embryo

Introduction

Since its start in January 2020, the COVID19 outbreak quickly reached pandemic proportions with a steep rise in mortality and mounting pressure on health services worldwide, as well as marked damage to the economy (Duan et al., 2020; Nicola et al., 2020). The pandemic has evidenced that our available repertoire of antiviral drugs is insufficient. Existing antiviral [remdesivir (Wang et al., 2020) and lopinavir/ritonavir (Kim et al., 2020; Lim et al., 2020)], anti-inflammatory [dexamethasone (Villar et al., 2020)], and immunomodulatory drugs [chloroquine (Borba et al., 2020), hydroxychloroquine (Meo et al., 2020; Sinha and Balayla, 2020), and ivermectin (Caly et al., 2020; Heidary and Gharebaghi, 2020)], have been proposed as treatment following clinical trials. However, except for dexamethasone, none of these drugs are currently recommended by the World Health Organization to treat COVID19 patients other than outside the context of clinical trials due to serious side effects (WHO, 2020). Despite this recommendation, remdesivir has already been approved in some countries for emergency use in patients with severe COVID19 symptoms, as it decreases the duration of hospitalization and shows a modest reduction of mortality rates in severely afflicted patients (Beigel et al., 2020). However, given that this drug costs 2,430 USD per treatment[1], it is unlikely to be a sustainable option for developing countries, such as those in Latin America, where the number of new COVID19 cases continues to grow steadily. With nearly 38 million confirmed infections worldwide and more than one million deaths at the time of writing this paper, the need for effective and safe options to treat COVID19 patients is urgent.

The surge in COVID19 cases and the lack of effective treatments have led to a growing number of informal reports and testimonials across social networks regarding the oral and intravenous use of

[1] https://www.gilead.com/news-and-press/press-room/press-releases/2020/6/an-open-letter-from-daniel-oday-chairman--ceo-gilead-sciences

chlorine dioxide (ClO_2) solution as an efficacious treatment of COVID19. In an unprecedented move, the Senate of Bolivia authorized the extraordinary use of ClO_2 to “manufacture, sell, supply and use ClO_2 to prevent and treat COVID19” (law PL N° 219/2019-2020 CS approved 15 July 2020). This situation has sparked concern from health agencies of various countries regarding the potential toxicity of using this disinfectant as a treatment, given that ClO_2 has strong oxidative properties. Chlorine dioxide, a gas that is highly soluble in water, has been known since 1946 for its broad antimicrobial properties (Sigstam et al., 2014), for which it is commonly used to purify water for human consumption, decontaminate produce and other food items (López-Gálvez et al., 2018), and disinfect surgical instruments (Doona et al., 2014). According to the Food and Drug Administration (FDA) of the US, consuming ClO_2 can lead to adverse effects such as 'vomiting, diarrhoea, dehydration, abdominal pain, metahemaglobinemia and systemic failures that could potentially lead to death'. However, an impartial review of the scientific peer-reviewed literature reveals few case reports of human patients presenting adverse effects after consumption of ClO_2, none of which were fatal, and in all cases reversed completely after treatment (Kishan, 2009; Bathina et al., 2013; Romanovsky et al., 2013; Loh and Shafi, 2014). Published studies on ClO_2 toxicity have reported null to mild effects in adult humans and other animals (e.g. Lubbers et al., 1982; Akamatsu et al., 2012; Ma et al., 2017) and have stressed that toxicity is strongly dose-dependent (Bercz et al., 1982; Hose et al., 1989; Ma et al., 2017). Interestingly, despite the voiced concerns, there are two drugs based on acidified sodium chloride (a precursor for generation of ClO_2, named NP001 and WF10) that have been used intravenously in humans to treat diverse conditions, including diabetic foot ulcer and amyotrophic lateral sclerosis (ALS), without reporting adverse reactions (Yingsakmongkol et al., 2011; Yingsakmongkol, 2013; Miller et al., 2015; Maraprygsavan et al., 2016).

The virucidal effect of ClO_2 when used as a disinfectant of water and hard surfaces is well documented. Specifically, there is evidence of virucidal activity against echovirus (Zhong et al., 2017), enterovirus (Jin et al., 2013), poliovirus (Simonet and Gantzer, 2006), rotavirus (Chen and Vaughn, 1990), norovirus (Lim et al., 2010; Montazeri et al., 2017), calicivirus (Montazeri et al., 2017), and coronavirus (Wang et al., 2005). However, to date, there are few publications that explore potential antiviral effects *in vitro* and *in vivo*. One of the few studies available found that mice that were exposed to influenza A virus in an environment that contained aerosolized ClO_2 had significantly lower mortality than mice that were solely exposed to Influenza A virus (Ogata and Shibata, 2008). The authors reported that the antiviral effect was due to denaturation of hemaglutinin and neuraminidase glicoproteins, a finding that concurs with previous studies that explain the virucidal mechanism of action of ClO_2 due to oxidation of amino acid residues that are key for cell entry (Noss and Olivieri, 1985; Ison et al., 2006; Stewart et al., 2008). More recently, the antiviral mechanism of action of ClO_2 was investigated *in vitro* using pig alveolar macrophages and MARC-145 cells exposed to the porcine reproductive and respiratory syndrome virus (PRRSV1), finding that the chemical also inhibits the synthesis of pro-inflammatory molecules that contribute to the pathogenesis of this disease (Zhu et al., 2019). The authors concluded that viral synthesis of RNA and proteins was impeded by ClO_2, leading to a reduction in viral replication. Despite these studies, to date there has been no published report of an *in vivo* assessment of the antiviral effect of ClO_2. Here, we have investigated the effect of a ClO_2 solution in 10-day old chick embryos inoculated with attenuated avian infectious bronchitis coronavirus (IBV) Massachusetts and Connecticut vaccine strains, which are pathogenic for birds during their embryonic stages of development (Tsai et al., 2016).

Methods

Chick embryo inoculation

We used 30 10-day old SPF RossxRoss chick embryos (Pilgrims, Mexico) incubated at 38°C and 65-70% humidity (Guy, 2015). Embryos were placed at random within the incubator to avoid any slight variation in humidity and temperature that could affect results. Prior to starting the experiment, all embryos were candled to ensure their viability, and were examined daily to search for evidence of death (presence of blood ring or lack of visible eggshell membrane blood vessels). Five chick embryos were assigned to each of the six experimental groups and treated accordingly (see Table 1). In all cases, embryos were inoculated via the chorioallanotic sac, as recommended for avian coronavirus replication (Jordan and Nassar, 1973; Escorcia et al., 2002). Before inoculation, the eggshell was disinfected with 70% ethanol and 3.5% iodine (Guy, 2015). Using the tip of sterile scissors, a hole was drilled in the eggshell over a 1 cm^2 transparent tape film and a sterile 1ml syringe with a 28-g 5/16" needle was used to administer the treatment directly into the allantoic cavity as indicated in Table 1. All procedures were carried out aseptically. After inoculation, the drilled hole was sealed with a drop of glue and the embryo was returned to the incubator. Inoculation of every embryo was performed by a single person to ensure experimental variation was kept at a minimum. Embryos were candled daily to determine mortality. As there was no death recorded within the first 24 h post-inoculation, none of the embryos were discarded from the experiment.

Macroscopic examination

Seven days after inoculation, embryos were sacrificed according to the American Veterinary Medical Association guidelines on humane treatment and euthanasia of chick embryos over 13 days of age (AVMA 2020). The embryos were placed at 4 °C for 4 h to ensure blood coagulation and avoid contamination of the allantoic fluid (Guy, 2015). Next, each egg was placed on a firm

surface with the air chamber facing upwards. The eggshell over the air chamber was disinfected with 70% ethanol and 3.5% iodine (Guy, 2015) and using sterile scissors, the eggshell and chorioallantoic membrane were removed to expose the allanotic fluid. A sterile pipette was used to aspirate 750 µl of the fluid and transfer it to a sterile cryovial before storage at −70 °C. Next, the embryo was removed from the eggshell using sterile dissection forceps and placed in a sterile Petri dish to be photographed.

Each embryo was cleaned with distilled water to remove any remaining albumin, vitellus and amniotic fluid before its mass was determined with a precision scale (±0.1 mg). Embryonic axis length was measured with digital callipers (± 0.1 cm). After decapitation with a sterile scalpel blade, each embryo was examined for macroscopic lesions typically caused by avian coronavirus, such as cutaneous haemorrhages, stunting, curving, urate deposits in the kidney and feather alterations (Escorcia et al., 2002; Alexander D.J. and D.A. Senne, 2008). Chick embryos were considered to have died during the experiment when there was evidence of disconnected or detached blood vessels of the chorioallantoic membrane or their organs exhibited imbibition of haemoglobin. Further evidence of mortality was determined by examining the presence of autolysis at microscopic examination.

For each chick embryo, both femurs were dissected and their length was determined and averaged with a digital calliper as a surrogate measure of chick development. We collected samples of all organs and tissues, including those known to be affected by the Massachusetts and Connecticut strains of avian coronavirus, namely trachea, lung, proventricle, duodenum, liver, kidneys and the Bursa of Fabricius (Escorcia et al., 2002; Cavanagh, 2003, 2007; Tsai et al., 2016), and those reportedly affected by exposure to ClO_2, namely thyroid (Bercz et al., 1982; Harrington et al., 1986), thymus, spleen and bone marrow (EPA, 2000).

148 Microscopic examination

149 Samples were cut longitudinally at their mid-section and immersed in 10% buffered formalin, pH
150 7.4. Fixed samples were paraffin-embedded and sectioned at 3 µm with a microtome before being
151 stained with haematoxylin-eosin for microscopic examination. The slides were observed under the
152 microscope at 40X and 100X.

153 To assess haematopoietic status, bone marrow preparations were used for a 200-cell differential
154 count to classify the marrow precursors and to determine the myeloid:erythroid (M/E) ratio for
155 each embryo. This ratio was obtained by dividing the sum of all the granulocytic cells by the sum of
156 all the erythrocytic cells (Schalm and Jain, 1986).

157 Virus quantitation by RT-qPCR

158 The virus was quantified in the allantoid fluid with an RT-qPCR protocol (Naguib et al., 2017).
159 Briefly, RNA was extracted by adding 700 µL of Trizol (Invitrogen) to 500 µL of each sample. The
160 sample was incubated for 10 min at ambient temperature. Next, 200 µL of chloroform were
161 added, mixed by inversion, and centrifuged at 12,000 g for 10 min at 4 °C. The aqueous phase was
162 transferred to a sterile microtube, and 500 µL of isopropanol were added. The sample was
163 centrifuged at 12,000 g for 10 min at 4 °C prior to decanting the supernatant. The pellet was
164 washed with 500 µL of cold 70% ethanol, centrifuged at 7,500 g for 5 min at 4 °C and the
165 supernatant was removed completely. The dry pellet was resuspended in 12 µL of nuclease-free
166 water and centrifuged at 7,500 g for 1 min at 4 °C. Quantity and quality of the extracted RNA was
167 examined in a Nanodrop (Qiagen) spectrophotometer and all samples were diluted to 35 ng/mL
168 RNA before retrotranscription.

169 cDNA synthesis was performed with oligo dT and MLV reversotranscriptase (Invitrogen)according
170 to the manufacturer's instructions. Briefly, we used 8 µL of RNA, 1 µL of Oligo DT (50 ng/µL), 1 µL of

10 mM dNTP and 2 µL of nuclease-free H_2O. The reactions were incubated at 65 °C for 5 min and placed on ice for 1 min. Seven µL of the kits cDNA synthesis mix, which contains 4 µL 5X First-Strand Buffer, 2 µL 0.1 M DTT and 1 µL RNAse and DNAse free H_2O, were added prior to mixing by pipetting and incubating at ambient temperature (~25 °C) for 2 min. We added 1 µL pf SuperScript II RT, mixed by pipetting and incubated at ambient temperature for 10 min. The reactions were incubated at 42 °C for 50 min and inactivated at 70 °C for 15 min. All cDNA samples were stored at -20°C until used.

A 100 bp fragment of the avian coronavirus N gene was amplified using primers IBV-pan_FW-1 (5'-CAG TCC CDG ATG CNT GGT A) and IBV-pan_RV (5'-CC TTW SCA GMA ACM CAC ACT) (Naguib et al., 2017). Quantitation was done with SYBR Green qPCR (Qiagen) in a real-time thermal cycler (CFX connect, Biorad) under the following protocol: 45 °C for 10 min, initial denaturation at 95 °C for 10 min and 35 cycles of 95 °C for 15 s, 52 °C for 15 s, and 68 °C for 30 s, with a final extension step at 68 °C for 10 min. We used a cDNA sample extracted from 500 µL of the vaccine as a positive control (the vaccine contained 10^4 mean embryo infective dose (EID_{50})/mL of coronavirus strains Massachusetts and Connecticut). A linear regression was used to calculate the correlation coefficient ($R^2 = 0.99$) and the slope value (b = -5.062) of the RNA copy number and Cq values using a 10-fold dilution of the vaccine (10^4 to 10^{-1}; see standard curve in Supplementary material). The number of viral RNA copies (hereafter viral load) was determined by comparing the Cq against this standard curve (Naguib et al., 2017). All cDNA samples were diluted 1:10 prior to running the qPCR assays.

Statistical analyses

Contingency tables were built to investigate differences in the number of dead *vs*. live chick embryos between experimental groups. The relative risk of developing virus-related lesions between treated and un-treated embryos was calculated using Fisher exact tests to estimate

194 significance. Body mass, morphometrics, viral load, and lesion severity were compared among
195 groups by one-way ANOVA and post-hoc Tukey HSD tests. All analyses were performed in R
196 version 3.6.3 (R Core Team, 2016). Contingency tables, Fisher exact p-values and odds ratios were
197 calculated with R package Epitools version 0.5-10.1.

198 Bioethics statement

199 This study was carried out in compliance with the American Veterinary Medical Association
200 (AVMA) guide for humane treatment of chick embryos and approved by the Autonomous
201 University of Queretaro Research Ethics Committee.

202

203 **Results**

204 Avian coronavirus RNA was detected in all of the embryos that were inoculated with the vaccine
205 (n=15, in all cases Cq <40). The viral load varied significantly between treatments (ANOVA;
206 $F_{2,12}$=4.421, p=0.036; Fig. 1), being 2.4 times higher in the untreated embryos. The average viral
207 load of ClO_2-treated chicks was $10^{4.3}$/mL, range: $10^{3.66} – 10^{5.03}$ and of untreated chicks was
208 $10^{4.83}$/mL, range: $10^{4.52} – 10^{5.01}$, respectively (Tukey HSD, Group E *vs*. F, p = 0.03). There were no
209 differences in the viral load between both ClO_2-treated groups (p>0.05).

210 Embryo mortality varied among groups (Fig. 2) and differed significantly between virus-inoculated
211 and virus-free embryos (Pearson's Chi^2 = 7.78; p = 0.004), reaching 80 % (4/5) of mortality in the
212 viral control group (Group F). In the groups that contained viral-inoculated embryos treated with
213 ClO_2, 1/5 (20 %) of the infected embryos in the low dosage group (Group D) and 2/5 (40 %) of the
214 infected embryos in the high dosage group (Group E) died. In the groups that were not infected

with the virus, there was only one death observed, in the group that received the high dosage of ClO_2 (Group C).

Body mass, embryonic axis length and femur length differed between the virus-inoculated and virus free-groups, regardless of ClO_2 treatment. All of the virus-inoculated embryos exhibited dwarfing and had, on average, 38% lower mass ($t = 21.15$, $df = 29.40$, $p = 2.2 \times 10^{-16}$; Fig. 3A), 10% shorter axis length ($t = 58.43$, $df = 29.26$, $p = 2.2 \times 10^{-16}$; Fig. 3B), and 20% shorter femur length ($t = 8.49$, $df = 23.34$, $p = 1.4 \times 10^{-8}$; Fig 3C) than the virus-free groups. When analysing growth in the virus-inoculated groups, mass was significantly higher in embryos that were treated with ClO_2 ($t = -2.74$, $df = 12.98$, $p = 0.017$). Body length of virus-inoculated chicks did not vary according to ClO_2 treatment ($p > 0.1$). See supplementary material for photographs of the embryos.

Lesions previously described in embryos infected with avian coronavirus were observed at post mortem examination. Namely, curling, the presence of white caseous material (urates), thickened amnion and allantoic membranes that adhered to the embryos, oedematous serous membranes, epidermal congestion, and subcutaneous haemorrhage (Table 2). Virus-inoculated embryos that were treated with ClO_2 had a lower risk of epidermal congestion (RR = 0.4; Wald 95% CI: 0.187-0.855; p = 0.04), haemorrhage (RR = 0.1; Wald 95% CI: 0.016 - 0.642; p = 0.002), curling (RR = 0.019; Wald 95% CI: 0.125 - 0.844; p = 0.017) and thickened membranes (RR = 0; p = 0.003) than untreated infected embryos. All the embryos had a pale liver and mildly congested lungs, regardless of their experimental group. Pale enlarged kidneys were observed in the virus-inoculated groups but not in the virus-free groups, regardless of ClO_2-treatment (see Table 2).

Microscopic lesions compatible with avian IBV infection were observed in various organs in all virus-inoculated groups (Fig. 4). The severity of the lesions was either similar or slightly lower in the embryos that had been treated with ClO_2 than in the embryos that did not receive any

238 treatment (Table 3). Two exceptions were the kidneys and the duodenum. In the kidneys, swelling
239 and degeneration of renal tubular epithelium was more common and more severe in the infected
240 chicks that were administered ClO_2 than in the infected embryos that did not receive ClO_2,
241 although the former presented mitotic cells. The duodenal villi of the embryos in the IBV-infected
242 groups were longer (ANOVA; $F_{5,18} = 5.62$, $p = 0.003$), and their base was wider (ANOVA; $F_{5,18} =$
243 13.65, $p = 1.39 \times 10^{-05}$) than embryos from the none-infected groups, and they were moderately
244 congested. Duodenal villous atrophy varied amongst groups (ANOVA; $F_{5,18} = 5.71$, $p = 0.003$) and
245 *post-hoc* comparisons revealed that the significant differences were E *vs.* B ($p = 0.021$) and E *vs.* C
246 ($p = 0.001$). The percent of bursal lymphoid tissue decreased markedly in the virus-inoculated
247 embryos (ANOVA; $F_{5,12} = 3.58$, $p = 0.033$; see Fig. 4). Virus-inoculated embryos showed mild
248 apoptosis in the thymus and heterophilic infiltration. Amongst the six experimental groups, all of
249 the embryos examined presented subacute heterophilic bursitis, and pulmonary interstitial
250 multifocal heterophilic foci with congestion (Table 3).

251 There were no observable alterations to the architecture and integrity of the tissues of non-
252 infected embryos that were administered ClO_2 (Experimental groups B and C), nor was any
253 difference in the area (μm^2) of the thyroid ($p>0.1$). ClO_2-treated groups showed a slightly higher
254 myeloid to erythroid ratio in the bone marrow than the experimental control group and the viral
255 control group, although the difference was not statistically significant (ANOVA; $F_{5,15} = 2.33$, $p =$
256 0.094).

257 **Discussion**

258 The use of chlorine dioxide (ClO_2) as a disinfectant is well established, and its virucidal effects are
259 reported against a wide range of enveloped and non-enveloped viruses that can affect human and
260 domestic animal health. To date, its informal use as an antiviral drug is polemical, and there are no

261 published studies that have explored the antiviral action of this substance following oral or
262 parenteral administration. We have investigated the antiviral effect of 30 ppm and 300 ppm ClO_2
263 solutions (both concentrations below the reported NOAEL; Bercz et al., 1982) in chick embryos
264 infected with avian infectious bronchitis coronavirus (IBV) strains. We observed a reduction in viral
265 titre in infected embryos that were treated with ClO_2. Mortality decreased substantially in the
266 ClO_2-treated embryos, although alterations to chick development were prevalent regardless of
267 treatment.

268 Virulent avian IBV strains typically have a burst size of 10 to 100 infective units per cell (Robb and
269 Bond, 1979), which appear in culture within six hours and can reach peak virus titres of $10^{6.5}$–$10^{8.5}$
270 $TCID_{50}$ after 36 hours (Otsuki et al., 1979). The vaccine strains used here have lower replication
271 efficiencies as they are attenuated (Tsai et al., 2020), but they are capable of replicating and
272 causing damage in chick embryos (Tsai et al., 2016). With 2,000 infective units (200 µl of 10^4
273 infective units/mL) inoculated into each embryo, the ClO_2 treatments decreased viral load 2.4-fold
274 compared to the infected non-treated embryos, representing an average difference of 42,711
275 infective units. This result could be explained by two mechanisms described for ClO_2. Firstly, direct
276 destruction or neutralization of the virions exposed to ClO_2, could have occurred due to
277 denaturing of their envelope glycoproteins following oxidation of amino acid residues(Noss and
278 Olivieri, 1985; Ison et al., 2006; Ogata and Shibata, 2008). Secondly, viral replication efficiency
279 could have decreased due to ClO_2–induced biochemical changes in the extra- or intracellular
280 milieu impeding the synthesis of viral RNA and proteins (see Enjuanes et al., 2006; Zhu et al.,
281 2019). These proposed mechanisms of action are not mutually exclusive.

282 The effects of reduced viral titres in the infected embryos were evident, with a 50 to 75%
283 reduction in mortality in the treated embryos treated with 300 ppm and 30 ppm of ClO_2,
284 respectively. However, developmental abnormalities were observed in the majority of the infected

285 embryos, including the groups that received ClO_2 treatment. Namely, dwarfing, assessed by body
286 mass, axis length, and femur length were significantly lower in all infected embryos, as expected to
287 occur in IBV infections (Balasubramaniam et al., 2013). In contrast, curling – also caused by avian
288 IBV (Wickramasinghe et al., 2011; Mork et al., 2014) – was virtually absent in the embryos that
289 received ClO_2 after infection. Alterations associated con IBV infection were observed in the
290 proventriculus, spleen, liver, but specifically in kidneys, trachea and lung. (Butcher et al., 1990;
291 Cook et al., 2012) were observed in most of the infected embryos, including those that were
292 administered ClO_2. However, for most of these abnormalities, severity was lower or similar in the
293 ClO_2-treated groups. One exception was the pathology observed in the kidneys, where lesions
294 indicative of nephrosis were more severe and frequent in the IBV-infected embryos treated with
295 ClO_2 than in the IBV-infected non-treated embryos. Such lesions in the kidneys are unlikely to be
296 due to the ClO_2 treatment itself, given that none of the non-infected embryos that were
297 administered ClO_2 showed any abnormality in the kidneys. Similarly, atrophy of the duodenal villi
298 was highest in the inoculated group that was administered a high dose of ClO_2, but absent in the
299 non-infected groups that only received ClO_2. If duodenal atrophy and nephropathogenicity in IBV-
300 infected embryos are mitigated by inflammatory responses (Chhabra et al., 2018), it is possible
301 that the observed tubular damage reflected ClO_2-driven downregulation of acute inflammation
302 that allowed virion replication in the tubular epithelium and in the duodenal villi. This scenario
303 could be plausible if we consider that a recent study that investigated the antiviral effect of ClO_2 in
304 pig alveolar macrophages and African green monkey kidney cells infected with the porcine
305 reproductive and respiratory syndrome virus (PRRSV1) *in vitro*, reported downregulation of pro-
306 inflammatory cytokines IL-1, IL-6 and TNF-α (Zhu et al., 2019). The drug NP001 (a chemical
307 precursor of ClO_2) exerts strong anti-inflammatory responses by inhibiting macrophage activation
308 in humans, even after a single dose (Miller et al., 2014). In turn, WF10, a strong oxidizing agent

309 that is related to ClO_2 (Veerasarn et al., 2004), induces apoptosis of inflammatory cells and
310 downregulates pro-inflammatory genes (Giese et al., 2004; Yingsakmongkol et al., 2011).
311 Interestingly, the affected renal tubules had mitotic cells, suggestive of regeneration as a
312 reparative response to damage of the renal tubular epithelium (Toback, 1992; Fujigaki, 2012;
313 Lombardi et al., 2016). This possibility will need to be explored further in the animal model used in
314 our study. Unfortunately, knowledge of IBV pathogenesis, immune responses and tissue
315 reparation in the embryonated egg is limited. In hatched birds, IBV can impact lymphocyte
316 populations by inducing apoptosis, thus impeding virus clearance (Caron, 2010). We found some
317 evidence of this effect, as the virus-inoculated embryos had a reduced percent of bursal lymphoid
318 tissue.

319 Taken together, our results indicate that ClO_2 limited viral replication but as the embryos were
320 only administered a single dose of a ClO_2 solution rather than repeated doses, not all virions were
321 eliminated. The viruses that remained viable after administration of the ClO_2 were able to
322 replicate, yielding lower viral titres, and the damage that they caused to the embryos was less
323 severe and ultimately led to less mortality than in the untreated infected embryos. Repeated
324 administrations of ClO_2 solution might have reduced the viral load further, plausibly leading to
325 even less virus-induced damage, a possibility that we could not explore in this model. However, an
326 important result of our study was the lack of evidence of tissue damage caused by ClO_2 itself. Only
327 one (20%) of the uninfected embryos treated with the high dose of ClO_2 died, and this difference
328 was not statistically significant to the experimental control. It is possible that the death was due to
329 other causes, as a 20% embryo mortality rate is considered normal in aviculture (Romanoff, 1972;
330 Fasenko & O´Dea, 2008).

331 Further studies should aim to test the antiviral effect of ClO_2 in hatched chicks, which have a more
332 mature immune system, and where repeated administrations are easier to procure. However, it is

promising that we found an evident effect against IBV without any significant adverse effect or evidence of toxicity to the chick embryos. Much research needs to be done before it is possible to generalize and extrapolate our findings to other viruses and animal hosts. However, in the context of the current COVID-19 crisis, with near to none viable, accessible and safe therapeutic option available, it might be prudent to consider conducting controlled double-blind and randomized studies on the antiviral effect of ClO_2 in COVID-19 patients.

Statement of conflict of interest

The authors declare they do not have any conflict of interest regarding this submission.

Funding

This research did not receive any specific grant from funding agencies in the public, commercial, or not-for-profit sectors.

Author contributions

K.A-W. and T.G-G. conceived the idea. K.A-W. supervised the experiments, performed statistical analyses and wrote the manuscript. X.Z-E. performed all gross examinations and histopathology analyses. C.D-S. conducted molecular assays and artwork. M.B-M. and F.G-D performed the inoculation experiments and assisted during necropsies. All authors participated in the discussion of results.

Acknowledgments

We thank Luis A. Soto-García and Karla Zamora y Cuevas for their help with photographic and video documentation of the experiment.

354 **References**

355 Akamatsu, A., Lee, C., Morino, H., Miura, T., Ogata, N., Shibata, T., 2012. Six-month low level
356 chlorine dioxide gas inhalation toxicity study with two-week recovery period in rats. J. Occup.
357 Med. Toxicol. 7, 2. doi:10.1186/1745-6673-7-2

358 Alexander D.J. and D.A. Senne, 2008. A Laboratory Manual for the Isolation, Identification and
359 Characterization of Avian Pathogens, American Association of Avian Pathologists.
360 ISBN:9780978916374

361 AVMA, 2020. Guidelines for the Euthanasia of Animals. American Veterinary Medicine Association.
362 ISBN:978-1-882691-54-8.

363 Balasubramaniam, A., Sukumar, K., Suresh, P., Puvarajan, B., 2013. Molecular characterisation of
364 membrane glycoprotein and 5b protein of nephropathogenic infectious bronchitis virus. Vet.
365 World. doi:10.14202/vetworld.2013.857-861

366 Bathina, G., Yadla, M., Burri, S., Enganti, R., Prasad Ch, R., Deshpande, P., Ch, R., Prayaga, A.,
367 Uppin, M., 2013. An unusual case of reversible acute kidney injury due to chlorine dioxide
368 poisoning. Ren. Fail. 35, 1176–1178. doi:10.3109/0886022X.2013.819711

369 Beigel, J.H., Tomashek, K.M., Dodd, L.E., Mehta, A.K., Zingman, B.S., Kalil, A.C., Hohmann, E., Chu,
370 H.Y., Luetkemeyer, A., Kline, S., Lopez de Castilla, D., Finberg, R.W., Dierberg, K., Tapson, V.,
371 Hsieh, L., Patterson, T.F., Paredes, R., Sweeney, D.A., Short, W.R., Touloumi, G., Lye, D.C.,
372 Ohmagari, N., Oh, M.-D., Ruiz-Palacios, G.M., Benfield, T., Fätkenheuer, G., Kortepeter, M.G.,
373 Atmar, R.L., Creech, C.B., Lundgren, J., Babiker, A.G., Pett, S., Neaton, J.D., Burgess, T.H.,
374 Bonnett, T., Green, M., Makowski, M., Osinusi, A., Nayak, S., Lane, H.C., 2020. Remdesivir for
375 the Treatment of Covid-19 - Final Report. N. Engl. J. Med. doi:10.1056/NEJMoa2007764

376 Bercz, J.P., Jones, L., Garner, L., Murray, D., Ludwig, D.A., Boston, J., 1982. Subchronic toxicity of
377 chlorine dioxide and related compounds in drinking water in the nonhuman primate.
378 Environ. Health Perspect. 46, 47–55. doi:10.1289/ehp.824647

379 Borba, M.G.S., Val, F.F.A., Sampaio, V.S., Alexandre, M.A.A., Melo, G.C., Brito, M., Mourão, M.P.G.,
380 Brito-Sousa, J.D., Baía-da-Silva, D., Guerra, M.V.F., Hajjar, L.A., Pinto, R.C., Balieiro, A.A.S.,
381 Pacheco, A.G.F., Santos, J.D.O., Naveca, F.G., Xavier, M.S., Siqueira, A.M., Schwarzbold, A.,
382 Croda, J., Nogueira, M.L., Romero, G.A.S., Bassat, Q., Fontes, C.J., Albuquerque, B.C., Daniel-
383 Ribeiro, C.T., Monteiro, W.M., Lacerda, M.V.G., 2020. Effect of High vs Low Doses of
384 Chloroquine Diphosphate as Adjunctive Therapy for Patients Hospitalized With Severe Acute
385 Respiratory Syndrome Coronavirus 2 (SARS-CoV-2) Infection: A Randomized Clinical Trial.
386 JAMA Netw. open. doi:10.1001/jamanetworkopen.2020.8857

387 Butcher, G.D., Winterfield, R.W., Shapiro, D.P., 1990. Pathogenesis of H13 nephropathogenic
388 infectious bronchitis virus. Avian Dis. 34, 916–921.

389 Caly, L., Druce, J.D., Catton, M.G., Jans, D.A., Wagstaff, K.M., 2020. The FDA-approved drug
390 ivermectin inhibits the replication of SARS-CoV-2 *in vitro*. Antiviral Res.
391 doi:10.1016/j.antiviral.2020.104787

392 Caron, L.F., 2010. Etiology and immunology of infectious bronchitis virus. Rev. Bras. Cienc. Avic.
393 doi:10.1590/S1516-635X2010000200007

394 Cavanagh, D., 2007. Coronavirus avian infectious bronchitis virus. Vet. Res. 38, 281–297.
395 doi:10.1051/vetres:2006055

396 Cavanagh, D., 2003. Severe acute respiratory syndrome vaccine development: experiences of
397 vaccination against avian infectious bronchitis coronavirus. Avian Pathol. 32, 567–582.

398 doi:10.1080/03079450310001621198

399 Chen, Y.S., Vaughn, J.M., 1990. Inactivation of human and simian rotaviruses by chlorine dioxide.
400 Appl. Environ. Microbiol. 56, 1363–1366. doi:10.1128/AEM.56.5.1363-1366.1990

401 Chhabra, R., Ball, C., Chantrey, J., Ganapathy, K., 2018. Differential innate immune responses
402 induced by classical and variant infectious bronchitis viruses in specific pathogen free chicks.
403 Dev. Comp. Immunol. 87, 16–23. doi:10.1016/j.dci.2018.04.026

404 Cook, J.K.A., Jackwood, M., Jones, R.C., 2012. The long view: 40 years of infectious bronchitis
405 research. Avian Pathol. 41, 239–250. doi:10.1080/03079457.2012.680432

406 Doona, C.J., Feeherry, F.E., Setlow, P., Malkin, A.J., Leighton, T.J., 2014. The Portable Chemical
407 Sterilizer (PCS), D-FENS, and D-FEND ALL: novel chlorine dioxide decontamination
408 technologies for the military. J. Vis. Exp. e4354. doi:10.3791/4354

409 Duan, H., Wang, S., Yang, C., 2020. Coronavirus: limit short-term economic damage. Nature.
410 doi:10.1038/d41586-020-00522-6

411 Enjuanes, L., Almazán, F., Sola, I., Zuñiga, S., 2006. Biochemical aspects of coronavirus replication
412 and virus-host interaction. Annu. Rev. Microbiol. 60, 211–230.
413 doi:10.1146/annurev.micro.60.080805.142157

414 EPA, 2000. Toxicological Review of Chlorine dioxide and Chlorite. CAS Nos. 10049-04-4 and 7758-
415 19-2. U.S. Environmental Protection Agency Washington, DC. http://www.epa.gov/iris.

416 Escorcia, M., Fortoul, T.I., Petrone, V.M., Galindo, F., López, C., Téllez, G., 2002. Gastric gross and
417 microscopic lesions caused by the UNAM-97 variant strain of infectious bronchitis virus after
418 the eighth passage in specific pathogen-free chicken embryos. Poult. Sci. 81, 1647–1652.
419 doi:10.1093/ps/81.11.1647

420 Fasenko, G.M., O´Dea, E.E., 2008. Evaluating Broiler Growth and Mortality in Chicks with Minor
421 Navel Conditions at Hatching. Poult. Sci. 87,594–597. doi: 10.3382/ps.2007-00352

422 Fujigaki, Y., 2012. Different modes of renal proximal tubule regeneration in health and disease.
423 World J. Nephrol. 1, 92–99. doi:10.5527/wjn.v1.i4.92

424 Giese, T., McGrath, M.S., Stumm, S., Schempp, H., Elstner, E., Meuer, S.C., 2004. Differential
425 effects on innate versus adaptive immune responses by WF10. Cell. Immunol. 229, 149–158.
426 doi:10.1016/j.cellimm.2004.08.001

427 Guy, J.S., 2015. Isolation and Propagation of Coronaviruses in Embryonated Eggs, in: Maier, H.J.,
428 Bickerton, E., Britton, P. (Eds.), Coronaviruses: Methods and Protocols, Methods in Molecular
429 Biology. Springer Protocols. New York. doi:10.1007/978-1-4939-2438-7_7

430 Harrington, R.M., Shertzer, H.G., Bercz, J.P., 1986. Effects of chlorine dioxide on thyroid function in
431 the African green monkey and the rat. J. Toxicol. Environ. Health 19, 235–242.
432 doi:10.1080/15287398609530923

433 Heidary, F., Gharebaghi, R., 2020. Ivermectin: a systematic review from antiviral effects to COVID-
434 19 complementary regimen. J. Antibiot. (Tokyo). doi:10.1038/s41429-020-0336-z

435 Hose, J.E., Di Fiore, D., Parker, H.S., Sciarrotta, T., 1989. Toxicity of chlorine dioxide to early life
436 stages of marine organisms. Bull. Environ. Contam. Toxicol. 42, 315–319.
437 doi:10.1007/BF01699954

438 Ison, A., Odeh, I.N., Margerum, D.W., 2006. Kinetics and mechanisms of chlorine dioxide and
439 chlorite oxidations of cysteine and glutathione. Inorg. Chem. 45, 8768–8775.
440 doi:10.1021/ic0609554

441 Jin, M., Shan, J., Chen, Z., Guo, X., Shen, Z., Qiu, Z., Xue, B., Wang, Y., Zhu, D., Wang, X., Li, J., 2013.

Chlorine dioxide inactivation of enterovirus 71 in water and its impact on genomic targets. Environ. Sci. Technol. 47, 4590–4597. doi:10.1021/es305282g

Jordan, F.T., Nassar, T.J., 1973. The combined influence of age of embryo and temperature and duration of incubation on the replication and yield of avian infectious bronchitis (IB) virus in the developing chick embryo. Avian Pathol. 2, 279–294. doi:10.1080/03079457309353804

Kim, J.-W., Kim, E.J., Kwon, H.H., Jung, C.Y., Kim, K.C., Choe, J.-Y., Hong, H.-L., 2020. Lopinavir-ritonavir versus hydroxychloroquine for viral clearance and clinical improvement in patients with mild to moderate coronavirus disease 2019. Korean J. Intern. Med. doi:10.3904/kjim.2020.224

Kishan, H., 2009. Chlorine dioxide-induced acute hemolysis. J. Med. Toxicol. Off. J. Am. Coll. Med. Toxicol.

Lim, J., Jeon, S., Shin, H.Y., Kim, M.J., Seong, Y.M., Lee, W.J., Choe, K.W., Kang, Y.M., Lee, B., Park, S.J., 2020. Case of the index patient who caused tertiary transmission of coronavirus disease 2019 in Korea: The application of lopinavir/ritonavir for the treatment of COVID-19 pneumonia monitored by quantitative RT-PCR. J. Korean Med. Sci. doi:10.3346/jkms.2020.35.e79

Lim, M.Y., Kim, J.-M., Ko, G., 2010. Disinfection kinetics of murine norovirus using chlorine and chlorine dioxide. Water Res. 44, 3243–3251. doi:10.1016/j.watres.2010.03.003

Loh, J.M.R., Shafi, H., 2014. Kikuchi-Fujimoto disease presenting after consumption of “Miracle Mineral Solution” (sodium chlorite). BMJ Case Rep. 2014. doi:10.1136/bcr-2014-205832

Lombardi, D., Becherucci, F., Romagnani, P., 2016. How much can the tubule regenerate and who does it? An open question. Nephrol. Dial. Transplant. Off. Publ. Eur. Dial. Transpl. Assoc. -

464 Eur. Ren. Assoc. 31, 1243–1250. doi:10.1093/ndt/gfv262

465 López-Gálvez, F., Randazzo, W., Vásquez, A., Sánchez, G., Decol, L.T., Aznar, R., Gil, M.I., Allende,
466 A., 2018. Irrigating Lettuce with Wastewater Effluent: Does Disinfection with Chlorine Dioxide
467 Inactivate Viruses? J. Environ. Qual. 47, 1139–1145. doi:10.2134/jeq2017.12.0485

468 Lubbers, J.R., Chauan, S., Bianchine, J.R., 1982. Controlled clinical evaluations of chlorine dioxide,
469 chlorite and chlorate in man. Environ. Health Perspect. 46, 57–62. doi:10.1289/ehp.824657

470 Ma, J.-W., Huang, B.-S., Hsu, C.-W., Peng, C.-W., Cheng, M.-L., Kao, J.-Y., Way, T.-D., Yin, H.-C.,
471 Wang, S.-S., 2017. Efficacy and Safety Evaluation of a Chlorine Dioxide Solution. Int. J.
472 Environ. Res. Public Health 14. doi:10.3390/ijerph14030329

473 Maraprygsavan, P., Mongkolsuk, J., Arnhold, J., Kuehne, F.-W., 2016. The chlorite-based drug
474 WF10 constantly reduces hemoglobin A1c values and improves glucose control in diabetes
475 patients with severe foot syndrome. J. Clin. Transl. Endocrinol. 4, 53–58.
476 doi:10.1016/j.jcte.2016.05.001

477 Meo, S.A., Klonoff, D.C., Akram, J., 2020. Efficacy of chloroquine and hydroxychloroquine in the
478 treatment of COVID-19. Eur. Rev. Med. Pharmacol. Sci. doi:10.26355/eurrev_202004_21038

479 Miller, R.G., Block, G., Katz, J.S., Barohn, R.J., Gopalakrishnan, V., Cudkowicz, M., Zhang, J.R.,
480 McGrath, M.S., Ludington, E., Appel, S.H., Azhir, A., 2015. Randomized phase 2 trial of NP001-
481 a novel immune regulator: Safety and early efficacy in ALS. Neurol. Neuroimmunol.
482 neuroinflammation 2, e100. doi:10.1212/NXI.0000000000000100

483 Miller, R.G., Zhang, R., Block, G., Katz, J., Barohn, R., Kasarskis, E., Forshew, D., Gopalakrishnan, V.,
484 McGrath, M.S., 2014. NP001 regulation of macrophage activation markers in ALS: a phase I
485 clinical and biomarker study. Amyotroph. Lateral Scler. Frontotemporal Degener. 15, 601–

609. doi:10.3109/21678421.2014.951940

Montazeri, N., Manuel, C., Moorman, E., Khatiwada, J.R., Williams, L.L., Jaykus, L.-A., 2017. Virucidal Activity of Fogged Chlorine Dioxide- and Hydrogen Peroxide-Based Disinfectants against Human Norovirus and Its Surrogate, Feline Calicivirus, on Hard-to-Reach Surfaces. Front. Microbiol. 8, 1031. doi:10.3389/fmicb.2017.01031

Mork, A.-K., Hesse, M., Abd El Rahman, S., Rautenschlein, S., Herrler, G., Winter, C., 2014. Differences in the tissue tropism to chicken oviduct epithelial cells between avian coronavirus IBV strains QX and B1648 are not related to the sialic acid binding properties of their spike proteins. Vet. Res. 45, 67. doi:10.1186/1297-9716-45-67

Naguib, M.M., El-Kady, M.F., Lüschow, D., Hassan, K.E., Arafa, A.-S., El-Zanaty, A., Hassan, M.K., Hafez, H.M., Grund, C., Harder, T.C., 2017. New real time and conventional RT-PCRs for updated molecular diagnosis of infectious bronchitis virus infection (IBV) in chickens in Egypt associated with frequent co-infections with avian influenza and Newcastle Disease viruses. J. Virol. Methods 245, 19–27. doi:10.1016/j.jviromet.2017.02.018

Nicola, M., Alsafi, Z., Sohrabi, C., Kerwan, A., Al-Jabir, A., Iosifidis, C., Agha, M., Agha, R., 2020. The socio-economic implications of the coronavirus pandemic (COVID-19): A review. Int. J. Surg. doi:10.1016/j.ijsu.2020.04.018

Noss, C.I., Olivieri, V.P., 1985. Disinfecting capabilities of oxychlorine compounds. Appl. Environ. Microbiol. 50, 1162–1164. doi:10.1128/AEM.50.5.1162-1164.1985

Ogata, N., Shibata, T., 2008. Protective effect of low-concentration chlorine dioxide gas against influenza A virus infection. J. Gen. Virol. 89, 60–67. doi:10.1099/vir.0.83393-0

Otsuki, K., Noro, K., Yamamoto, H., Tsubokura, M., 1979. Studies on avian infectious bronchitis

508 virus (IBV). II. Propagation of IBV in several cultured cells. Arch. Virol. 60, 115–122.
509 doi:10.1007/BF01348027

510 R Core Team, 2016. R Development Core Team. R A Lang. Environ. Stat. Comput.

511 Robb, J.A., Bond, C.W., 1979. Coronaviridae, in: Fraenkel-Conrat, H., Wagner, R.R. (Eds.),
512 Comprehensive Virology. Springer, Boston. doi:https://doi.org/10.1007/978-1-4684-3563-
513 4_3

514 Romanoff, A., Romanoff, A., 1972. Spontaneous malformations, in: Romanoff, A.L. (Ed.),
515 Pathogenesis of the avian embryo: an analysis of causes of malformations and prenatal
516 death. Wiley-Interscience, New York. ISBN:978-0471732402

517 Romanovsky, A., Djogovic, D., Chin, D., 2013. A case of sodium chlorite toxicity managed with
518 concurrent renal replacement therapy and red cell exchange. J. Med. Toxicol. Off. J. Am. Coll.
519 Med. Toxicol. 9, 67–70. doi:10.1007/s13181-012-0256-9

520 Schalm, O.W., Jain, N.C., 1986. Schalm's veterinary hematology, 4th editio. ed. Lea & Febiger,
521 Philadelphia.

522 Sigstam, T., Rohatschek, A., Zhong, Q., Brennecke, M., Kohn, T., 2014. On the cause of the tailing
523 phenomenon during virus disinfection by chlorine dioxide. Water Res. 48, 82–89.
524 doi:10.1016/j.watres.2013.09.023

525 Simonet, J., Gantzer, C., 2006. Degradation of the Poliovirus 1 genome by chlorine dioxide. J. Appl.
526 Microbiol. 100, 862–870. doi:10.1111/j.1365-2672.2005.02850.x

527 Sinha, N., Balayla, G., 2020. Hydroxychloroquine and covid-19. Postgrad. Med. J.
528 doi:10.1136/postgradmedj-2020-137785

529 Stewart, D.J., Napolitano, M.J., Bakhmutova-Albert, E. V, Margerum, D.W., 2008. Kinetics and

mechanisms of chlorine dioxide oxidation of tryptophan. Inorg. Chem. 47, 1639–1647. doi:10.1021/ic701761p

Toback, F.G., 1992. Regeneration after acute tubular necrosis. Kidney Int. 41, 226–246. doi:10.1038/ki.1992.32

Tsai, C.-T., Tsai, H.-F., Wang, C.-H., 2016. Detection of infectious bronchitis virus strains similar to Japan in Taiwan. J. Vet. Med. Sci. 78, 867–871. doi:10.1292/jvms.15-0609

Tsai, C.-T., Wu, H.-Y., Wang, C.-H., 2020. Genetic sequence changes related to the attenuation of avian infectious bronchitis virus strain TW2575/98. Virus Genes 56, 369–379. doi:10.1007/s11262-020-01753-5

Veerasarn, V., Khorprasert, C., Lorvidhaya, V., Sangruchi, S., Tantivatana, T., Narkwong, L., Kongthanarat, Y., Chitapanarux, I., Tesavibul, C., Panichevaluk, A., Puribhat, S., Sangkittipaiboon, S., Sookpreedee, L., Lertsanguansinchai, P., Phromratanapongse, P., Rungpoka, P., Trithratipvikul, S., Lojanapiwat, B., Ruangdilokrat, S., Ngampanprasert, P., 2004. Reduced recurrence of late hemorrhagic radiation cystitis by WF10 therapy in cervical cancer patients: a multicenter, randomized, two-arm, open-label trial. Radiother. Oncol. J. Eur. Soc. Ther. Radiol. Oncol. 73, 179–185. doi:10.1016/j.radonc.2004.05.007

Villar, J., Añón, J.M., Ferrando, C., Aguilar, G., Muñoz, T., Ferreres, J., Ambrós, A., Aldecoa, C., Suárez-Sipmann, F., Thorpe, K.E., Jüni, P., Slutsky, A.S., Ferrando, C., Mellado-Artigas, R., Fernández, J., Hernández, M., Castellá, M., Castro, P., Badia, J.R., Aguilar, G., Carbonell, J.A., Badenes, R., Tornero, C., Ferreres, J., Blasco, M.L., Carbonell, N., Serrano, A., Juan, M., Gómez-Herreras, J.I., López, M.L., Ambrós, A., Martín, C., Del Campo, R., Puig-Bernabeu, J., Ferrer, C., De Andrés, J., Muñoz, T., Serna-Grande, P., Tamayo, G., Martínez-Ruíz, A., Bilbao-Villasante, I., Villar, J., Fernández, R.L., Calvo, C.P., Vidal, Á., Añón, J.M., Figueira, J.C., Asensio,

M.J., Maseda, E., Suárez-Sipmann, F., Ramasco, F., Varela-Durán, M., Díaz-Parada, P., Trenado-Álvarez, J., Fernández, M.M., Aldecoa, C., Rico-Feijoo, J., Fernández, L., Sánchez-Ballesteros, J., Blanco-Schweizer, P., Martínez, D., Soler, J.A., Slutsky, A.S., Jüni, P., Thorpe, K.E., Thomas, R., Wysocki, K., De Verno, P., Lakhanpal, G., Juando-Prats, C., 2020. Efficacy of dexamethasone treatment for patients with the acute respiratory distress syndrome caused by COVID-19: Study protocol for a randomized controlled superiority trial. Trials. doi:10.1186/s13063-020-04643-1

Wang, X.-W., Li, J.-S., Jin, M., Zhen, B., Kong, Q.-X., Song, N., Xiao, W.-J., Yin, J., Wei, W., Wang, G.-J., Si, B.-Y., Guo, B.-Z., Liu, C., Ou, G.-R., Wang, M.-N., Fang, T.-Y., Chao, F.-H., Li, J.-W., 2005. Study on the resistance of severe acute respiratory syndrome-associated coronavirus. J. Virol. Methods 126, 171–177. doi:10.1016/j.jviromet.2005.02.005

Wang, Yeming, Zhang, D., Du, G., Du, R., Zhao, J., Jin, Y., Fu, S., Gao, L., Cheng, Z., Lu, Q., Hu, Y., Luo, G., Wang, K., Lu, Y., Li, H., Wang, S., Ruan, S., Yang, C., Mei, C., Wang, Yi, Ding, D., Wu, F., Tang, X., Ye, X., Ye, Y., Liu, B., Yang, J., Yin, W., Wang, A., Fan, G., Zhou, F., Liu, Z., Gu, X., Xu, J., Shang, L., Zhang, Y., Cao, L., Guo, T., Wan, Y., Qin, H., Jiang, Y., Jaki, T., Hayden, F.G., Horby, P.W., Cao, B., Wang, C., 2020. Remdesivir in adults with severe COVID-19: a randomised, double-blind, placebo-controlled, multicentre trial. Lancet. doi:10.1016/S0140-6736(20)31022-9

Wickramasinghe, I.N.A., de Vries, R.P., Gröne, A., de Haan, C.A.M., Verheije, M.H., 2011. Binding of avian coronavirus spike proteins to host factors reflects virus tropism and pathogenicity. J. Virol. 85, 8903–8912. doi:10.1128/JVI.05112-11

WHO, 2020. Corticosteroids for COVID-19. World Health Organization. WHO/2019-nCoV/Corticosteroids/2020.1. https://www.who.int/publications/i/item/WHO-2019-nCoV-

576 Corticosteroids-2020.1

577 Yingsakmongkol, N., 2013. Clinical outcomes of WF10 adjunct to standard treatment of diabetic
578 foot ulcers. J. Wound Care 22, 130-132,134-136. doi:10.12968/jowc.2013.22.3.130

579 Yingsakmongkol, N., Maraprygsavan, P., Sukosit, P., 2011. Effect of WF10 (immunokine) on
580 diabetic foot ulcer therapy: a double-blind, randomized, placebo-controlled trial. J. foot ankle
581 Surg. Off. Publ. Am. Coll. Foot Ankle Surg. 50, 635–640. doi:10.1053/j.jfas.2011.05.006

582 Zhong, Q., Carratalà, A., Ossola, R., Bachmann, V., Kohn, T., 2017. Cross-Resistance of UV- or
583 chlorine dioxide-resistant echovirus 11 to other disinfectants. Front. Microbiol. 8, 1928.
584 doi:10.3389/fmicb.2017.01928

585 Zhu, Z., Guo, Y., Yu, P., Wang, X., Zhang, X., Dong, W., Liu, X., Guo, C., 2019. Chlorine dioxide
586 inhibits the replication of porcine reproductive and respiratory syndrome virus by blocking
587 viral attachment. Infect. Genet. Evol. J. Mol. Epidemiol. Evol. Genet. Infect. Dis. 67, 78–87.
588 doi:10.1016/j.meegid.2018.11.002

589 Figures

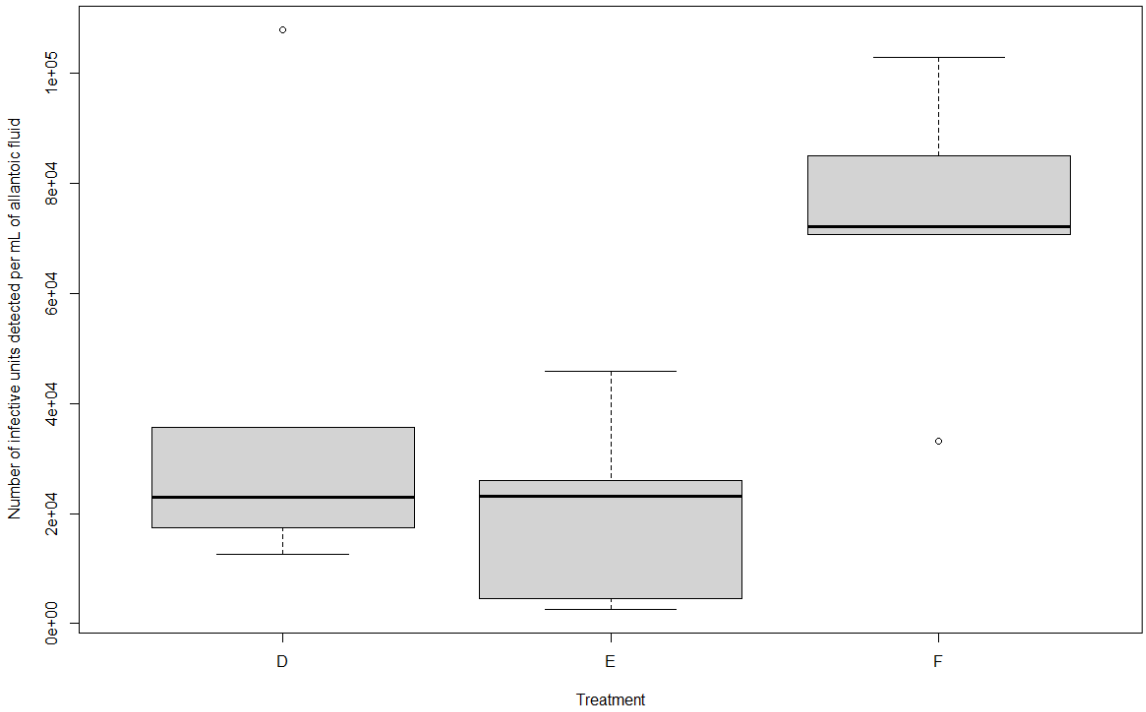

590

591 **Figure 1.** Virus RNA copy number in the allantoic fluid of the infected embryos per treatment group. Virus

592 copy number was calculated by the geometric mean of the triplicate Cq value referred to the standard curve

593 (see methods). Experimental groups D to F contained virus-inoculated embryos (D: Low dose of ClO_2, E: High

594 dose of ClO_2, F. Viral control). For details on treatments, see Table 1.

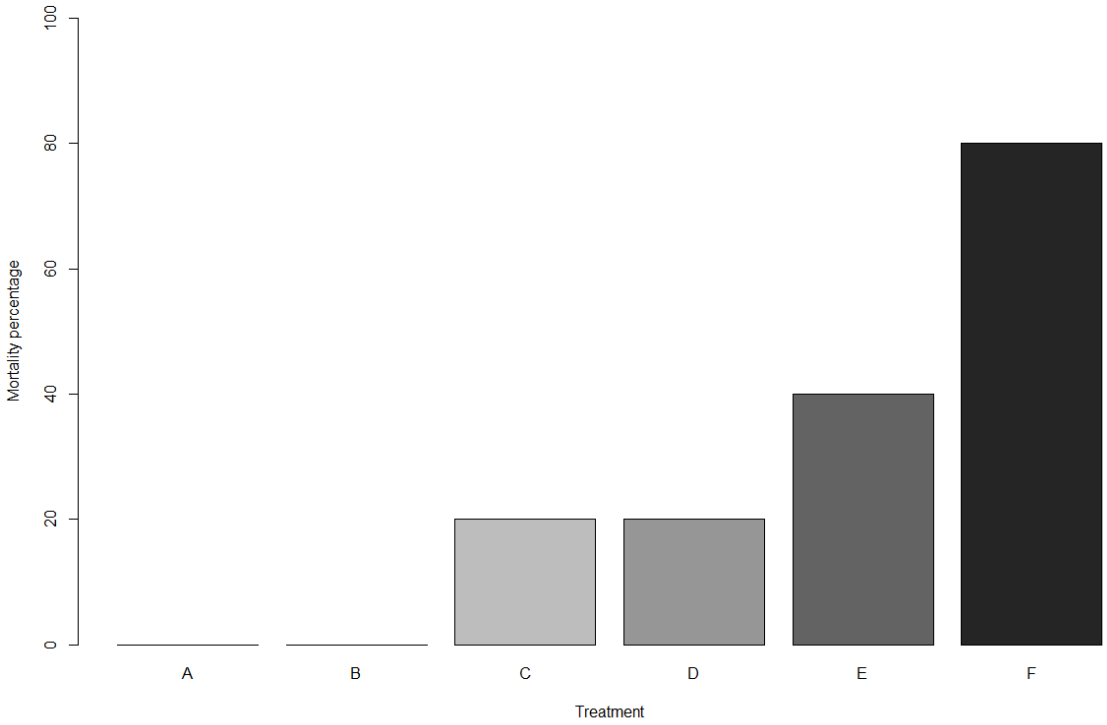

Figure 2. Chick embryo mortality during the experiment. Experimental groups A to C contained virus-free embryos (A: Experimental control, B: Low dose of ClO_2, C: High dose of ClO_2); experimental groups D to F contained virus-inoculated embryos (D: Low dose of ClO_2, E: High dose of ClO_2, F. Viral control). For details on treatments, see Table 1.

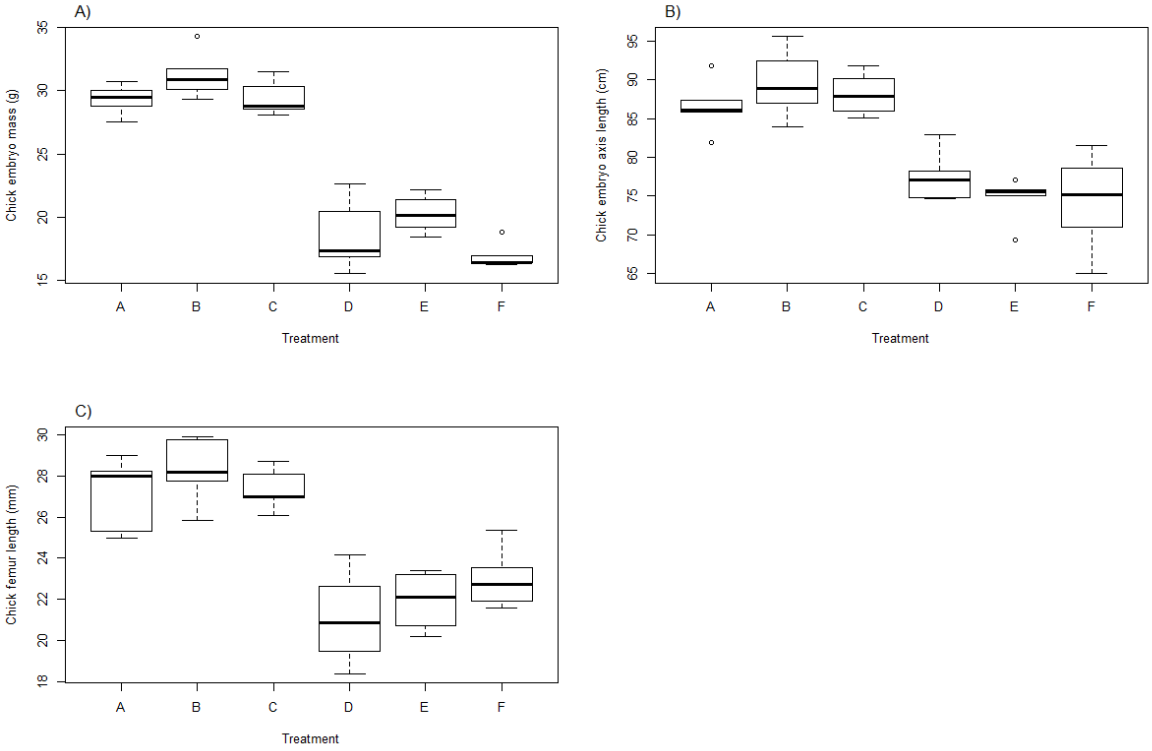

600

601 **Figure 3.** Chick embryo development at the end of the experiment (day 17 of incubation). A) mass, B) body

602 axis, C) femur length. Experimental groups A to C contained virus-free embryos (A: Experimental control,

603 B: Low dose of ClO_2, C: High dose of ClO_2); experimental groups D to F contained virus-inoculated embryos

604 (D: Low dose of ClO_2, E: High dose of ClO_2, F. Viral control). For details on treatments, see Table 1.

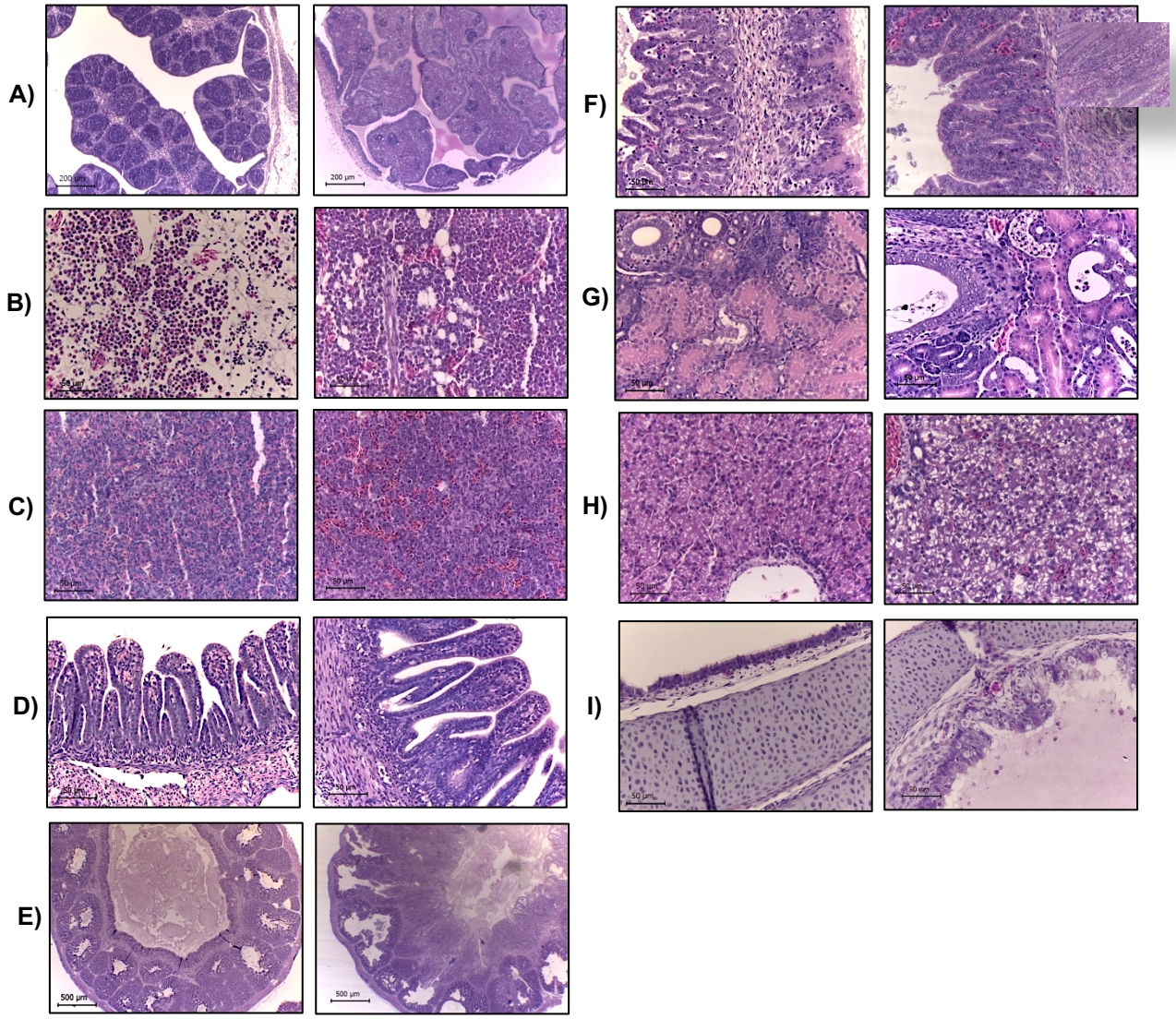

Figure 4. Histology of selected tissues from 17-day-old chick embryos. In each row, microphotograph pairs show H&E-stained representative tissues of non-infected (left) and infected embryos (right), A) Bursa of Fabricio (100X). Infected embryos showed severe lymphoid depletion, with approximately 10% of active lymphoid tissue and abundant heterophils. B) Bone marrow (400 X). Infected embryos showed an increase in erythroid cellularity ne, C) Spleen (400 X), Infected embryos showed reticuloendothelial hyperplasia, D) Duodenum (400 X). Infected embryos showed mild villous atrophy, E) Proventricle (40X). Infected embryos showed epithelial hyperplasia with desquamation and hyaline material, F) Proventricle (400X). Image shows the increased length of the proventricular folds and mitotic cells indicative of epithelial

627 regeneration, G) Kidney (400X). Infected embryos showed swelling, cell detritus and protein within the

628 tubules, and basophilic material compatible with urate crystals, H) Liver (400X). Infected embryos showed

629 glucogenic degeneration, I) Trachea (400X). Infected embryos showed hyperplasia and epithelial

630 degeneration. Scale = 50 µm in all panels except for E (scale = 500 µm).

Table 1. Experimental groups used to assess the *in vivo* antiviral effect of high and low concentrations of ClO2 solution in chick embryos. The table shows the number of embryos included in each group. (LD: Low dose, HD: High dose)

Group	N	Treatment
Group A (Experimental control)	5	200 µl of sterile 0.9% saline solution
Group B (ClO_2 LD)	5	100 µl of sterile ClO_2 solution (30 ppm[1]) and 100 µl of sterile 0.9% saline solution
Group C (ClO_2 HD)	5	100 µl of sterile ClO_2 solution (300 ppm[2]) and 100 µl of sterile 0.9% saline solution
Group D (Virus + ClO_2 LD)	5	100 µl of resuspended avian coronavirus vaccine and 100 µl of sterile ClO_2 solution (30 ppm)
Group E (Virus + ClO_2 HD)	5	100 µl of resuspended avian coronavirus vaccine and 100 µl of sterile ClO_2 solution (300 ppm)
Group F (Viral control)	5	100 µl of resuspended live attenuated avian coronavirus vaccine (Bron Blen® Merial, containing 10^4 of mean embryo infective dose (EID_{50})/mL of coronavirus strains Massachusetts and Connecticut) and 100 µl of sterile 0.9% saline solution

[1] This concentration is 10 times below the no-observed-adverse-effect level (NOAEL; 3.5 mg/kg per day) determined for ClO_2 (Bercz et al. 1982), considering an embryonic mass of 10 g at the time of inoculation.
[2] This concentration is equal to the NOAEL considering an embryonic mass of 10 g at the time of inoculation.

Table 2. Macroscopic abnormalities observed at necropsy in the chick embryos. The table shows the number of embryos in each group that presented each lesion. (LD: Low dose, HD: High dose)

	Dwarfing	Curling	White caseous material	Thickened membranes	Oedema	Epidermal congestion	Pale and enlarged kidneys
Group A (Experimental control)	0/5[f]	0/5[f]	0/5[f]	0/5[f]	0/5	0/5[f]	0/5
Group B (ClO_2 LD)	0/5[f]	0/5[f]	0/5[f]	0/5[f]	0/5	0/5[f]	0/5
Group C (ClO_2 HD)	0/5[f]	0/5[f]	1/5[f]	0/5[f]	0/5	2/5	0/5
Group D (Virus + ClO_2 LD)	5/5[a]	1/5	1/5[f]	0/5[f]	0/5	2/5	5/5[f,a]
Group E (Virus + ClO_2 HD)	5/5[a]	0/5[f]	1/5[f]	0/5[f]	0/5	2/5	3/5[a]
Group F (Viral control)	5/5[a]	4/5[a]	4/5[a]	4/5[a]	1/5	5/5[a]	1/5

634

[a]: Indicates a significant difference to the experimental control

[f]: Indicates a significant difference to the viral control

Table 3. Microscopic abnormalities related to avian coronavirus infection in the chick embryos. (LD: Low dose, HD: High dose)

	A (Exp. control)	B (ClO_2 LD)	C (ClO_2 HD)	D (Virus + ClO_2 LD)	E (Virus + ClO_2 HD)	F (Viral control)
Trachea	-	Mild hyperplasia	Mild hyperplasia	Karyorexis, focal hyperplasia	Moderate congestion	Mild hyperplasia
Lung	Mild to moderate congestion	Moderate congestion, interstitial oedema	Mild to moderate congestion, interstitial oedema	Moderate to severe congestion, karyolysis	Mild to moderate congestion, moderate oedema	Mild to moderate congestion, severe to moderate oedema
Proventricle	-	-	-	Moderate hyperplasia	Mild hyperplasia	Moderate hyperplasia, mild congestion
Duodenum	-	-	-	Moderate congestion		Mild diffuse congestion, atrophy of intestinal villi
Liver	-	-	-	Gluogenic degeneration, mild congestion	Gluogenic degeneration, mild congestion	Gluogenic degeneration, moderate congestion, periportal eosinophilic material
Kidneys	-	-	-	Degeneration w/ regeneration, congestion, mild heterophilic infiltration, urates	Degeneration w/ regeneration, congestion, mild heterophilic infiltration, urates	Haemorrhage, multifocal heterophilic infiltration, urates
Spleen	-	-	-	Reticuloendothelial hyperplasia	Reticuloendothelial hyperplasia	Reticuloendothelial hyperplasia
Bursa of Fabricius	Subacute heterophilic bursitis	Subacute heterophilic bursitis	Subacute heterophilic bursitis	Subacute heterophilic bursitis	Subacute heterophilic bursitis	Subacute heterophilic bursitis